Proceedings of the 14th International Conference on Nuclear Engineering
IMECE
November 9-15, 2012, Houston, Texas, USA

IMECE2012-87834

PASSIVE EVAPORATIVE COOLER FOR MALARIA TESTING IN DEVELOPING COUNTRIES

Briana Lucero-Bernhardt
Colorado School of Mines
Golden, CO, USA

Cameron Turner
Colorado School of Mines
Golden, CO, USA

ABSTRACT

A top-wicking cooler box was designed for this purpose and included an experimental and theoretical analysis of an evaporative cooling technique utilizing mounted water troughs and a single transfer surface. Construction and insulation material, cooling capabilities, and environmental sustainability were compared between two boxes with different dimensions. The smaller boxes were found to be more effective due to a smaller ratio of volume to surface area, which resulted in higher cooler system effectiveness than the larger boxes. Regardless of the roofing metal, it was found that the square dimensioned boxes were unsuitable to sufficiently cool numerous RDTs irrespective of their scaling. Future testing on rectangular boxes and additional evaporative cooling options warrant further investigation.

INTRODUCTION

Sub-tropical climates are plagued with finding feasible solutions to combat mosquito-carried diseases such as malaria. These malaria-endemic communities require a passive evaporative cooler box to store rapid diagnostic test (RDTs) kits without the use of electricity at temperatures below 25°C.

Researchers at the Colorado School of Mines became aware of the need to develop a passive cooler box for employment with rapid detection test kits (RDTs) in Africa in 2009. The RDTs were developed and are utilized by The Foundation for Innovative New Diagnostics (FIND), a non-government organization (NGO) located in Geneva Switzerland, to cost-effectively and accurately diagnose malaria cases across the globe.

Malaria is an infectious disease transmitted by mosquitoes in humid climates by blood borne parasites. It is estimated that approximately half the population of the world was exposed to malaria across 109 countries in 2008 (Munoz et al., 2009). The most effective method of combating malaria is prevention. Tools such as mesh bed netting, insecticidal sprays, and knowledge and prophylaxis drugs have been invaluable in the battle. The symptoms of malaria; high fevers and body aches, span the indications of numerous diseases and cannot be used alone as a diagnosis. For a precise diagnosis, laboratory testing and microscopic blood examinations must be employed. The RDTs fall into the category of laboratory tests and provide the most inexpensive option available. Much in the same vein as pregnancy tests, the RDTs allow for short diagnosis times but are susceptible to rapid aging in high ambient relative humidity and temperature.

The RDTs need to be stored at temperatures under 25°Celsius and lower levels of relative humidity in order to retain their diagnosing abilities. In many malaria-endemic communities, electricity is not easily accessible and is expensive; thus posing a threat to current methods of sustaining the RDTs at recommended temperatures. In an attempt to rectify this issue and reach more rural communities, "cooler boxes" have been requested to house multiple RTDs.

This project was a continuation of a Senior Design project under the Humanitarian Engineering minor program. The Senior Design team designed, constructed and tested several methods of passive cooling before settling on one specific model (Munoz et al. 2009). This specific box was a 0.305 m x 0.305 m x 0.457 m (1ft x 1ft x 1.5 ft) cooling box that utilized evaporative cooling through a top-wicking device and was found to be the most efficient and cost effective option for maintaining acceptable temperatures and relative humidity levels for the RTDs. Early prior research demonstrated the superiority of ceramics for bearings (1, 2) and the existence of elasto- hydrodynamic (ehd) lubricant films at ball and roller contacts (3), the calculation of which is now an accepted part of bearing engineering. These new concepts are now used in the design of lubrication systems with solid lubricants that operate in much more severe environments than oils and greases (4, 5). Proprietary computer codes and unique patented bearing

configurations for optimizing the performance of bearing/solid-lubricant systems have been developed (6, 7 and 8). In this way, patented self-contained solid-lubricated all-steel and hybrid-ceramic ball and roller bearings are now available for environments that do not contribute to their lubrication, such as in air or vacuum.

As a continuation of the project, two larger 0.610m x 0.610m x 0.762m (2ft x 2ft x 2.5ft) boxes have been constructed and tested which will hold at least 40 RDT boxed units with shelves. The roofing material of the two boxes was varied to include copper and aluminum. The smaller evaporative box, previously developed by the Senior Design team was modified to utilize the same insulating material, used in the two larger boxes, and as tested should hold at least 6 RDT box units.

Sustainability Definition

For the purposes of this study, sustainability is in reference to the environmental, economic and social consequences of the construction of these cooler boxes. Environmentally, the boxes should have as small an ecological footprint as possible. This means that the quantity and types of resources used during the materials acquisition, manufacture, transportation, construction, use and disposal should be minimized. These resources include the land needed to mine the metal and the fuel required to operate the processing plant of the insulation, as well as the technology used to develop the processes.

The economic sustainability is a measurement of the sustained welfare of a community as a result of the production or consumption of a given product. In theory, the product should not diminish any persons' ability to enjoy health, wealth or utility. Therefore it is closely related to the social consequences since the goal is to provide social justice, peace and security to all the citizens involved with the production, consumption and/or disposal of the product (Mulder, 2006).
The economic consequences in this case can be intertwined with the social consequences. Since the boxes will be labor intensive to fabricate and construct, they will require the employment of a skilled workforce. This will brings jobs to the local economy and provide a sense of community ownership. Additionally, since the RDT units will test for malaria, one social benefit can be measured by the number of people diagnosed with the aid of this technology.

Design Requirements

The final box design shall meet the following requirements:

- $T_{inside} < 25^{o}C$, when $T_{ambient} \leq 40^{o}C$
- Holds 10 RDT units (RDTs 76.2mm x152.4mm x63.5mm each)
- Passive - no external power required
- Interior dimensions - 0.4572m x 0.4572m x 0.4572m
- Cost of production < $100/per unit
- Low maintenance – easy to use and repair
- Manufactured with locally available tools, labor and materials (though materials could be made available for manufacturing purposes.)
- Adaptable design for use in different environments

BACKGROUND AND RELATED WORKS APPROACH

Experimental Description

The Senior Design team provided a promising box design that was found to be a square evaporative cooler box (Munoz, et al., 2009). The boxes are insulated on 5 sides with 50.8mm Mylar coated polymethyl methacrylate roof foam insulation panels (R13 insulation value). One of the vertical wall panels contains a notched door that latches to access the interior on the larger boxes as seen in Figure 1. The top of the boxes are enclosed by a metal roof, either made of copper or aluminum. At the intersection of the roof and the insulation, the boxes have been sealed with expanding foam insulation sealer. For the smaller box, the door has been omitted, with access to the inside of the box being available through a removable roof.

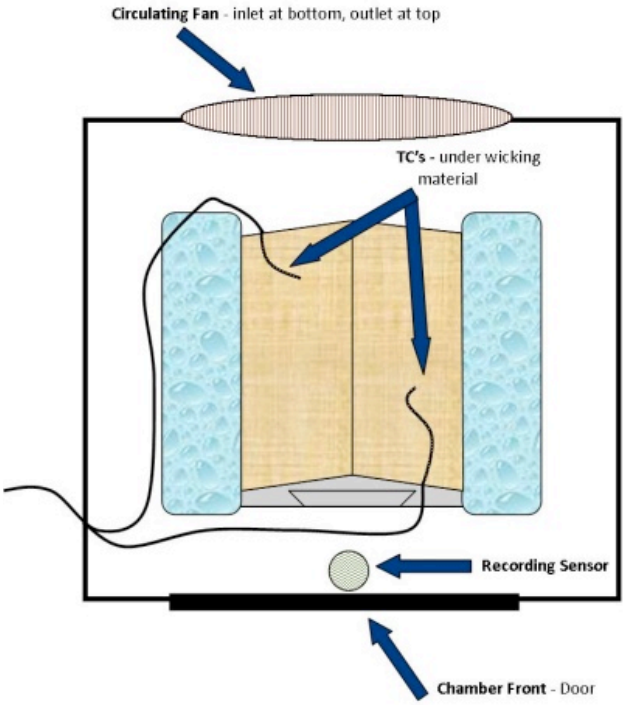

Figure 1 Test set-up to simulate operation in clinic

The wicking material utilized was a commercially available Shamwow® fabric manufactured in Germany. The synthetic cloth most closely resembles felt when dry, and silk when wet. It was selected because of its ability to pull water from the troughs up to the pitch of the roof. Other materials such as cotton and linen were originally tested by the Senior Design team on the small box and did not wick to the full extent of the roof. For this reason, the Shamwow® material was the best material option available. For the larger boxes several

sheets of the Shamwow® material were sewn together to cover the roof entirely.

Testing was performed at the Denver Federal Center in a 4 foot square Russells Technical Products (Model PD-64-3, Serial Number 0286440) environmental test chamber. This test chamber had the capabilities of controlling its internal temperature and humidity from -10 to 170°C and 10 to 95 % relative humidity. The boxes were placed inside the chamber with the RDT access door facing the door of the chamber. The back side of the boxes faced the back of the chamber where a radial blower is driven by a 1750 RPM AC motor. The motor drives a squirrel cage blower and circulates air from the bottom (inlet) to the top of the chamber (outlet). Therefore the air generated by the fan was blowing across the pitch of the roof. The boxes were centered in the chamber with an equal distance from the sides of the chamber.

The complete system has two wall-paper trays attached as rain gutters might be attached to the roof of a house. These trays hold the water and a submersed piece of the wicking material that also covers the roof and allows for the evaporation. During the box operation, these trays are braced by wooden supports that allow the user to control the level of the trays to allow for constant wicking. They are also covered with aluminum foil to reduce excess evaporation into the chamber. This setup allows the water to continually wet the wicking material and cool the box. The wicking material utilized is Shamwow sheets sewn together to fit the shape of the roof.

To measure the temperature of the roof, two thermocouples (TCs) were attached to each side of the roof pitch. Using these T-type TCs, the exterior roof temperature beneath the wicking material was recorded and used in the theoretical simulations. To reduce the thermal contact resistance, silicone grease was placed between the thermocouple ends and the metal roof. From these measurements, the surface temperature on the top of the wicking material was calculated. These surface temperatures were used to find the effectiveness of the boxes.

The temperature and relative humidity of both the ambient conditions and the internal box conditions were recorded with LASCAR EL-USB-2+ relative humidity/temperature sensors. The ambient conditions sensors were placed between the front of the box and the chamber access door. The internal conditions sensors were placed inside the boxes on the floor just slightly inside the door in an upright position. The box doors were then shut and latched. For all the tests the sensors sampled the temperature and relative humidity once every minute.

Testing of the system consisted of 1 hour ramping times and 5 hour dwell times at each temperature and relative humidity. The temperatures were varied from 25-45^{o}C with relative humidity varied from 30%-90%. The experimental test matrix can be found in Table 1. During the test, the relative humidity was held constant while the temperature was varied for each of the three humidity sets. Therefore each test consisted of three "sets" of tests with three different temperatures and three different relative humidities.

Table 1 Design Matrix

Trial	Temperature (°C)	% Relative Humidity
1	25	30
2	35	30
3	45	30
4	25	60
5	35	60
6	45	60
7	25	90
8	35	90
9	45	90

Box Modification

During the 4th week of testing, it was decided that the boxes were not performing as well as expected. Several contributors to the lack of performance were considered to be the cardboard sides, the insulation seams, the door and the roof-to-wall intersections. All of these concerns were addressed and modified to ensure a greater seal was obtained.

Accordingly, the cardboard sides were removed to reveal the outside insulation since warping of the cardboard from the high relative humidities was occurring. No insulation damage was observed as a result the past tests or the humidity. Upon removal of the warped material it was evident that there were some significant gaps in the insulation construction. Several cans of the expanding foam insulation were used to seal along all insulation seams, roof seams and interior seams.

As another main contributor to potential heat gains to the cooled space, the doors were also revamped. The insulation was grooved to accept the protrusions placed in the doors. This meant that the copper box had to have the entire front face replaced as there was not enough room to groove the door. For the hardware on the door, plastic strips were placed on either side of the foam. This was done to ensure that the hardware did not puncture the Mylar coating of the foam and compromise the thermal integrity of the box.

Thermal Model Description

Theoretical modeling of the system has been accomplished and the results were compared to the experimental data. Using EES software, the objective was to find the Shamwow® outer surface temperature that provides an energy balance of the cooling effects and the various heat gains. In an attempt to find the surface temperature manually, calculations were also performed in Excel employing the Newton-Raphson root finding method to solve the resulting transcendental, non-linear energy balance. The schematic in Figure 2 shows the heat exchange within the system as modeled and calculated. It should be noted that the contact resistance between the wicking material and the metal roof has been included in the wet cloth resistance of the wicking material.

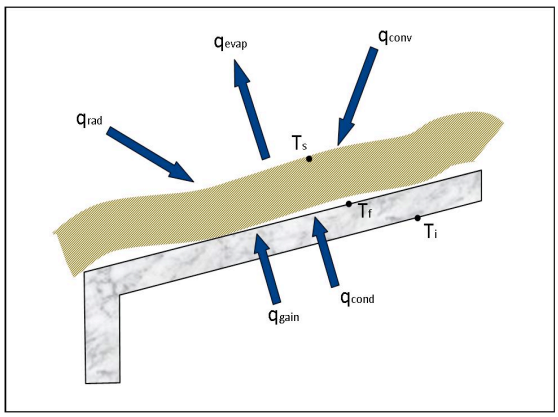

Figure 2 Heat exchange diagram

Several assumptions were made in the process of calculating the heat balance of the system. These have been outlined below:

- Steady-state conditions
- Dry air behaves as an ideal gas
- Constant properties, except for variable specific volume in temperature range of interest
- For the radiation exchange calculations, the wicking material surface is small in comparison to the large, isothermal surroundings (inside surfaces of the environmental chamber)
- No heat loss/gain occurs from any surface other than roof; all other box surfaces are considered adiabatic.
- Internal convection can be neglected
- Contact resistance between wicking and cooling surface is included in the resistance of the wet cloth (wicking material).
- The external metal roof surface temperature (T_f) is equivalent to the internal metal roof temperature (T_i) since the roof thickness is so thin (0.001m) and the corresponding thermal resistance is small

The resistive schematic of the system is shown in Figure 3 as the heat transfer across the box top surface (Incropera et al., 2007). Therefore the internal air temperature is assumed to be that of the inside metal roof surface temperature. And the metal temperature T_f and T_i are equivalent because of the small metal thickness and the relatively high thermal conductivity yields a very small thermal resistance.

Since the top surface of the Shamwow® material is where the evaporation occurs, this temperature is the focal point of the system. The evaporation is the driving force of heat transfer that decreases the internal box temperature. The metal portions of the upper wall ends were omitted from the calculations for simplification.

Evaporation is the result of a phase change from a liquid water to water vapor mixed with air. On the molecular level, evaporation occurs when the water molecules on the surface of a liquid develop sufficient kinetic energy to overcome the attractive forces between the liquid molecules and join the air molecules as vapor. The dry bulb temperature is defined as the measured air temperature value not impacted by the amount of moisture in the air. The wet bulb temperature is that achieved when liquid water is cooled by evaporation in an equilibrium process. The wet-bulb temperature must be less than the dry-bulb temperature for evaporation to occur (Sonntag et al., 2003).

The energy needed to generate a phase change without a change in temperature is better known as the latent heat. It expresses the amount of heat energy required to create a phase change of a given unit of mass without altering the system temperature. Sensible heat is the amount of heat used to increase the temperature of a substance. Evaporation is then the conversion of sensible heat to latent heat. Non-saturated air is cooled by heat and mass transfer. More heat and mass transfer can occur by forcing the movement of more air across a saturated water surface area using fans or natural ventilation. A portion of the air's sensible heat is transferred to the water, where it becomes latent heat by evaporation (Camargo et al., 2005; Incropera et al., 2007).

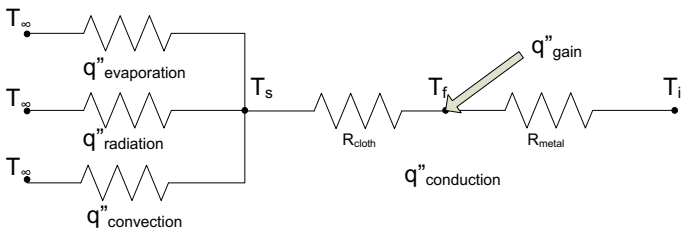

Figure 3 Surface resistance schematic

The mixed convection heat transfer is composed of both free (natural) and forced convection. The forced convection is an externally driven flow within the ambient air. The natural convective flow is driven by buoyancy forces that act as a result of the gravity vector and is directed with normal and parallel components along the inclined roof surface. Figure 4 qualitatively shows the buoyancy driven flow across the roof where the normal force is in the y-direction. Since the plate is being cooled, the buoyancy force maintains the descending flow. The component of the gravitational acceleration in the direction parallel to the roof line (x-direction) is dependent on the pitch angle θ and results in a reduction of the convective heat transfer from this surface below that for a vertical plate (Sonntag et al., 2003; Incropera et al., 2007).

For the sake of model simplicity, the convective heat transfer of the box interior has been neglected. However it is important to understand how the air will cool the RDT box units since convection is a significant heat transfer mode within the insulated box. On the inside of the box, the buoyant convective flow adds heat to the internal surface (T_i). A pictorial representation can be found in Figure 4 where the colder air at the internal roof surface is gradually replaced by warmer air in a natural convective cycle from the bottom of the box. This heat transfer between the internal box air and the roof decreases the dry-bulb temperature of the air. The lowest temperature possible with evaporative cooling is the outside ambient wet bulb temperature. These are small temperature

differences, especially in high humidity areas, therefore it is not possible to fill the box completely since there will need to be some air movement around the boxed units.

A recommended packing scheme would ideally have at least 25 mm between the insulation walls and the RDT units and between the RDT units themselves. If 2 shelves were placed inside the large boxes at approximately 152 mm interval spacing from the floor, 4 RDT units could be placed on each shelf. These shelves would ideally be 0.25 m in length to allow for the internal convection to reach the units on the bottom of the box. With this shelf set-up then 40 units could be placed on the floor in 4 rows, 3 deep and stacked 2 high. Thus the shelves provide an opportunity to greatly increase the number of units cooled.

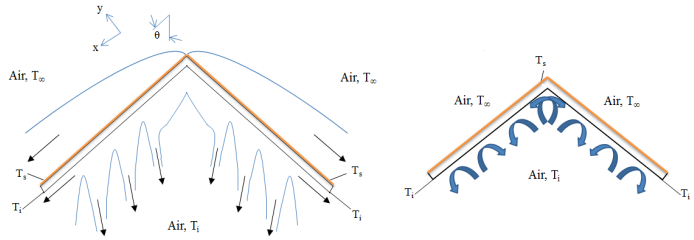

Figure 4 Buoyancy flow across box roof (Incopera et al., 2007)

It is known that the mixture density decreases with increasing temperature. However, the increasing relative humidity also causes a decrease in the mixture density. The mixture density is calculated using the relative humidity and the ambient temperature as seen in equation (1) (Sonntag et al., 2003).

$$\rho_{mixture} = \frac{P_a}{RT}\left(0.622\frac{P_g}{P_a}+1\right) \quad (1)$$

These properties are shown graphically in Figure 5 where the higher temperature and humidity air is associated with lower mixture densities. Therefore, a buoyant flow could also be driven by a humidity difference. Because of the geometry, this flow would be directed in the opposite direction as that driven by the thermally driven buoyant flow.

The sensitivity of the mixture density to temperature and relative humidity changes were evaluated and plotted in Figure 5. It is evident that the temperature plays a more significant role in the mixture density than the relative humidity. The mixture density difference is greater by one order of magnitude over the range of temperature and relative humidity covered in the tests, meaning temperature is the main contributor to the mixture density. Therefore the buoyancy forces associated with the relative humidity difference between the top of the boundary layer of the Shamwow® material the ambient conditions were neglected.

Both the EES (commercially available Engineering Equation Solver) and the Excel Newton-Raphson (Newton-Raphson is a mathematical algorithm used to find the roots of transcendental equations) numerical models were developed from the physical models shown in Figures 2 through 4. The equations for this energy balance can be seen in Equations 2 through 7 below. A surface energy balance was performed on the upper surface of the wicking material. The convection, conduction, gain and radiation are all additive heat flux terms. The evaporation is the only term that provides cooling to the roof and therefore to the entire cooler box. The conduction is active through the metal surface and the wicking material. Whereas the radiation and convection (both free and forced) fluxes act on the upper surface of the Shamwow®. Equation 6 is transcendental primarily because of the nonlinearities associated with the radiation term (Equation 3) and the variable specific volume of the saturated vapor at the Shamwow® upper surface.

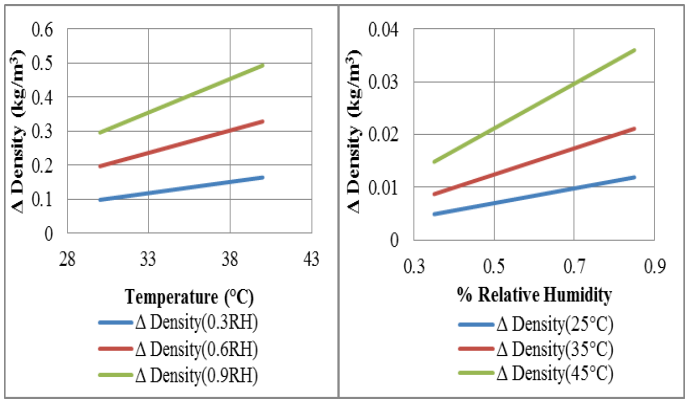

Figure 5 (a) Temperature difference of buoyancy forces at top of boundary layer (b) Relative humidity difference of buoyancy forces at top of boundary layer

$$q_{cond} = \frac{T_s - T_f}{R_{cloth}} + \frac{T_f - T_i}{R_{conduct}} \quad (2)$$

$$q_{rad} = \sigma\epsilon_{felt}(T_\infty^4 - T_s^4) \quad (3)$$

$$q_{convec} = h_{hx}(T_\infty - T_s) \quad (4)$$

$$q_{evap} = h_m h_{fg,water,s}(\rho_{water\ vapor,s} - \phi_\infty \rho_{water\ vapor,\infty}) \quad (5)$$

$$q_{cond} + q_{rad} + q_{convec} + q_{gain} = q_{evap} \quad (6)$$

$$\epsilon = \frac{T_\infty - T_i}{T_\infty - T_s} \quad (7)$$

The effectiveness for each of the boxes was calculated from Equations 2-7, where T_∞ is the ambient temperature, T_s is the Shamwow® external surface temperature, and T_i is the box internal temperature. The surface temperatures were calculated using both the EES and Newton-Raphson methods and plugged into the equation for system effectiveness. The ambient and internal temperatures were gathered from the USB data logger as the experimental temperatures of the actual boxes.

Life Cycle Assessment (LCA)

A Life Cycle Assessment (LCA) has been conducted assuming a lifespan of 5 years. Through this evaluation the choice and quantity of materials has been verified using the material lists available in SimaPro©, a commercially available life cycle assessment computer program. Both large boxes were analyzed with the same materials, but with different metals to

account for the different roofs. The LCA was performed using European data assuming that the majority of the external material would be shipped from this location. Since the small aluminum box is not functional for holding a sufficient number of RDTs, no LCA was performed on this box.

The two large boxes were assessed with the materials weights and descriptions found in Table 2. The only difference between these analyses is the copper and the aluminum roofing material. The roofs were constructed of metal sheeting that was primarily pure metal rolled out to the thickness of 1 mm. The metal angles used as the support of the box were steel coated in a thin layer of zinc to avoid oxidation. The polymethyl methacrylate foam sheets were cut down to fit directly into the steel/zinc braces. Once the foam walls were in place, the polyurethane expanding foam was used to fill in the cracks and ensure a proper seal. As cooler box fabricators gain experience in building these boxes, it is anticipated that the need for this large a mass of expanding foam would decrease.

Table 2 LCA Material Inputs

Material Description	Copper Quantity (kg)	Aluminum Quantity (kg)
Aluminum sheet, secondary, from scrap, at plant/RER	-	4.5
Copper sheet, secondary, from scrap, at plant/RER	3	-
Steel, chromium steel 18/8 at plant/RER	3.76	3.76
Zinc, primary, at regional storage/RER S	0.5	0.5
Polymethyl methacrylate, sheet, at plant/RER	2	2
Polyurethane flexible foam	1	1
Foam, expanding	1	1

RESULTS

Experimental Results

The results were gathered in 54 hour test increments that span the three different relative humidities and three temperatures. The data was analyzed in individual relative humidity or temperature tests independent of the other two recorded sets. The internal data averages are based on the ambient temperature plateaus and are placed in tables per each test and box type. Overall there was a positive temperature gradient from the ambient to the internal box conditions. However there were several cases, primarily at the higher temperatures and relative humidities, where there was a negative gradient where the internal temperature was greater than the ambient. The most effective boxes were the post-helium coolers with the best sealing. A single test of each post-helium box was conducted. If time had permitted, two replicates of the tests would have been conducted to allow improved statistical analysis.

Since there were two control variables (temperature and relative humidity) that were tested at three different levels, an Analysis of Variance was used to evaluate the data collected during testing (Frigon et al., 1997; Montgomery, 1997). This analysis tool allows for the evaluation of the variance within the data based on the independent variable (ambient temperature and humidity) and their levels and measures their significance. It also provides an estimate of the population variance based on the difference between the individual independent variable means. It essentially is a technique for decomposing the total variation observed across the experiments into the sources of variation. The sources of variation are important factors since they have an effect on the product performance and are included in this investigation. Analysis of Variance (ANOVA) provides a total variability of the experiment in a quantified form of an equation. From this equation the numerical variation in the data can be compared to the controlled variation of the temperature and relative humidity variables. Thus the quality of the experimental model can be verified (Otto et al., 2001). For this paper, the data was analyzed at a 90% percent confidence interval. To perform the analysis, the data at the ambient values laid out in Table 1 were averaged and graphed.

As the tests came to completion, the data was collected and analyzed using an ANOVA Design of Experiments approach. From this analysis it was determined that the temperature delta between the ambient conditions and the surface temperature contributed to the interior temperature more than the relative humidity delta.

The three boxes were compared using the current interior dimensions to determine the surface area to volume ratio. As seen in Figure 6, the large boxes have a surface area to volume ratio of approximately 53 using the internal dimensions; while the small box has a ratio of 110. The smaller ratio of the large boxes indicates that there are greater constraints in the available cooling surface area when scaling to larger boxes.

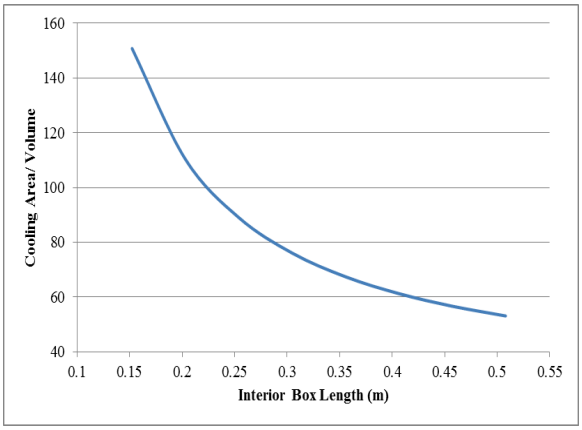

Figure 6 Constructed interior box length to cooling surface area to volume ratio

Because the surface area to volume ratio decrease with geometrically scaled size, an analysis for a box that would increase the ratio while still allowing for the greatest amount of interior space was developed. Assuming that the constructed roofs would be recycled for future use, the height of the boxes was then optimized to increase the surface area to volume ratio. The resulting box is a 0.610 m x 0.610 m x 0.381 m (2 ft x 2 ft x 1.25 ft) with a smaller vertical reach. Figure 7 shows the ideal dimensions where the ratio decreases with an increase in the wall height. If the recommended box were built and tested, the cost of material would decrease and the potential for cooling

capabilities increases. At the suggested height, the cooler box would be able to cool at least 20 RDT boxed units while the taller boxes can cool at least 40 RDT units with shelves.

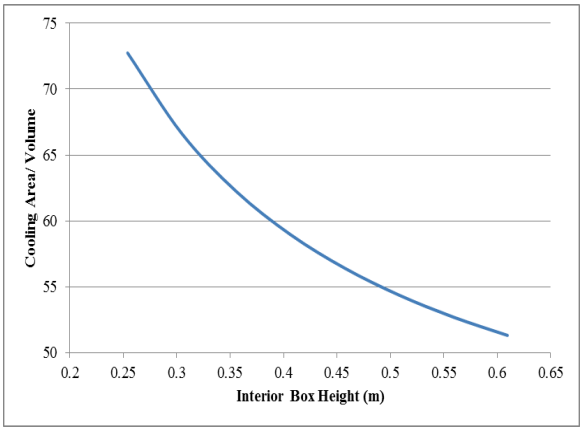

Figure 7 Idealized box height to cooling surface area to volume ratio

While one box was being tested in the anticipated final configuration, the other box was being tested for leaks using the sniffer and helium. Following the seam sealing with more foam, those boxes were tested. The boxes were in their final states and provided the most accurate picture of the effectiveness available for this study. With the gaps sealed, the copper test was run first. The results are plotted in Figures 8 through 9 and the raw data is shown in Table 3. There is a slightly greater temperature difference from the final design tests than the pre-helium tests.

At an ambient temperature of 25°C and relative humidities up to approximately 40%, the copper box will suffice to retain the RDTs at the desired 25°C temperature. However at the highest temperature and lowest relative humidity, the box will perform as a cooler box, though the internal temperatures are above those desired by the client. The greatest temperature difference can be found at the highest ambient temperature and lowest relative humidity, resulting in an over 8°C difference. While the temperatures above 30°C are not ideal for keeping the RDTs functional, this demonstrates that the evaporative potential of the box design will offer some cooling capacity in lower to moderate relative humidity cases.

The aluminum box also has the larger temperature gradient of over 9°C at the highest ambient temperature and lowest relative humidity. In the aluminum box though the higher temperatures is now showing a slight temperature gradient despite the humidities that show the evaporative process is still functioning. This is impressive as most of the other tests, including the small box tests resulted in values that were almost equal with the ambient conditions. In comparing the copper and the aluminum boxes, the aluminum has a slightly lower temperature (<1%) for all the testing conditions. This is likely due to differences in the box construction.

Table 3 Post-helium average test data

Test	Internal		Ambient		ΔT
	Temperature (°C)	Humidity (%RH)	Temperature (°C)	Humidity (%RH)	
Post-Helium Copper	22.5	69.4	25.8	60.2	3.3
	29.3	66.7	34.6	48.5	5.3
	36.2	59.3	44.4	36.7	8.2
	24.7	66.9	26.2	59.1	1.4
	31.5	74.5	35.6	61.7	4.1
	40.6	76.5	44.4	61.3	3.8
	26.4	87.0	25.5	94.5	-1.0
	34.3	95.0	34.8	95.9	0.5
	43.7	96.2	43.6	93.2	-0.1
Post-Helium Aluminum	21.4	66.9	24.7	63.5	3.3
	28.0	71.1	34.3	53.3	6.4
	34.7	69.4	44.4	39.8	9.8
	23.5	68.0	25.3	61.0	1.8
	29.8	74.8	34.4	61.9	4.5
	38.8	78.0	44.3	61.9	5.6
	26.9	81.5	25.3	92.8	-1.6
	33.8	87.9	34.8	95.4	1.1
	43.7	91.0	44.5	96.2	0.8

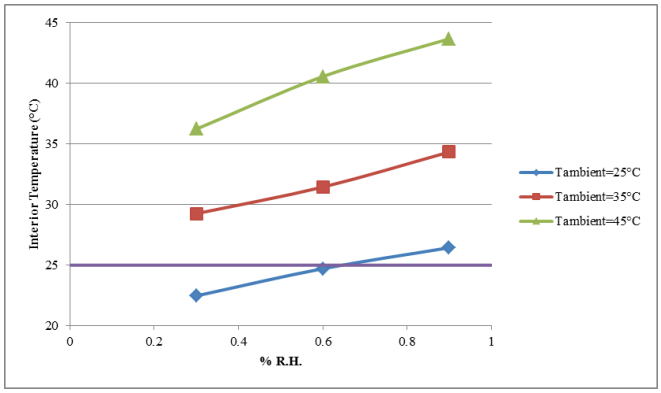

Figure 8 Copper post-helium test data

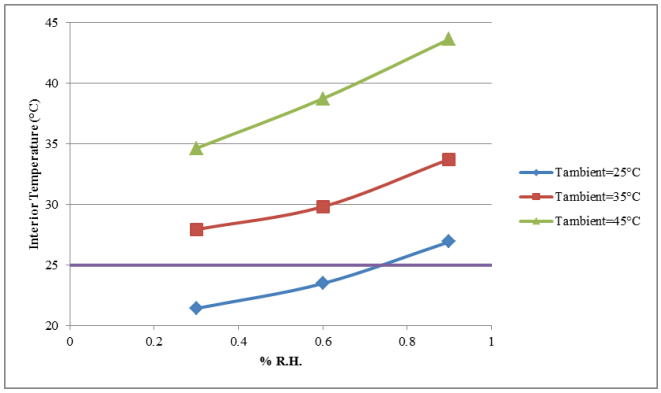

Figure 9 Aluminum post-helium test data

Thermal Analysis Results

The effectiveness of the two boxes can be seen in Tables 4 and 5 below. At the lowest relative humidity tested and the lowest temperature, the greatest effectiveness for the copper box and the second greatest for the aluminum box were seen. The greatest effectiveness for the aluminum box was seen at an ambient relative humidity of 60% and the median temperature. As the ambient temperature and relative humidity increased, the effectiveness of both boxes decreased.

A comparison of the surface temperatures (T_s) from the two set of calculations can be seen in Figures 10 and 11 with the average internal temperature (T_i) from the post-helium tests. At lower temperatures the EES calculations are undershooting the actual performance while the Newton Raphson calculations overshoot the performance. At the median ambient temperature, the Newton Raphson calculations are very similar to the data curve while the EES calculations continue to undershoot the performance. And at the highest ambient temperature, both calculations sets undershoot the predicted values. This shows that at higher temperatures, any leaks that were present become more prevalent with a greater temperature gradient resulting in higher heat gains from the cooling interior. The differences may be partially attributed to the temperature dependent property capabilities of the EES calculations in comparison to the manual Excel calculations. Within the Excel calculations only the specific volume of the saturated vapor for the saturated air at the edge of the boundary layer was calculated as a function of Shamwow® surface temperature, T_s. All other thermo physical properties were assumed constant.

Table 4 Copper post-helium effectiveness

Copper Post-helium Effectiveness				
$T_{ambient}$ (°C)	T_s (°C)	T_i (°C)	Ambient %R.H.	ε
25.78	22.00	22.48	60.25	0.87
34.56	25.99	29.26	48.54	0.62
44.39	31.47	36.24	36.68	0.63
26.16	23.91	24.72	59.10	0.64
35.60	29.29	31.46	61.72	0.66
44.42	36.52	40.57	61.35	0.49
25.46	27.86	26.45	94.52	0.41
34.83	32.35	34.34	95.91	0.20
43.61	41.06	43.69	93.17	-0.03

Table 5 Aluminum post-helium effectiveness

Aluminum Post-helium Effectiveness				
$T_{ambient}$ (°C)	T_s (°C)	T_i (°C)	Ambient %R.H.	ε
24.71	21.02	21.44	63.47	0.89
34.35	25.62	27.95	53.28	0.73
44.42	31.30	34.65	39.75	0.74
25.25	23.47	23.50	61.01	0.98
34.36	28.88	29.83	61.87	0.83
44.34	36.34	38.77	61.94	0.70
25.30	22.00	26.93	92.80	-0.50
34.84	31.94	33.75	95.36	0.38
44.47	40.89	43.65	96.20	0.23

In order to account for the heat gains of the system, a constant value of 600 W/m^2 was added to all calculations. This power flux gain is based on the area of the pitched roof cooling surface to be consistent with the other flux terms in the surface energy balance. This was done in the attempt to more closely model the measured interior temperature values of the tested boxes. At the higher temperatures then, a greater heat gain constant would have to be used to create a better curve fit. If the thermal conductivity of the wicking material were altered, it was observed that the slope of the theoretical curves was altered.

A thermal model of the system without the gain flux can be seen below in Figures 12 and 13. These theoretical curves can be considered the performance that could be achieved with no additional heat gain from the box walls or door. By performing a conduction shape factor analysis, it was possible to estimate the gain associated with heat conduction through the wall and floor insulation. Table 7 shows the amount of heat flux gained from an improperly sealed box based on the average ambient and internal temperature difference as measured in the post helium tests. As the ambient temperature increases, the amount of heat gained at the surface balance also increases from conduction through the insulated walls and floor. This would explain why the calculated curves are much lower at the lower ambient temperatures.

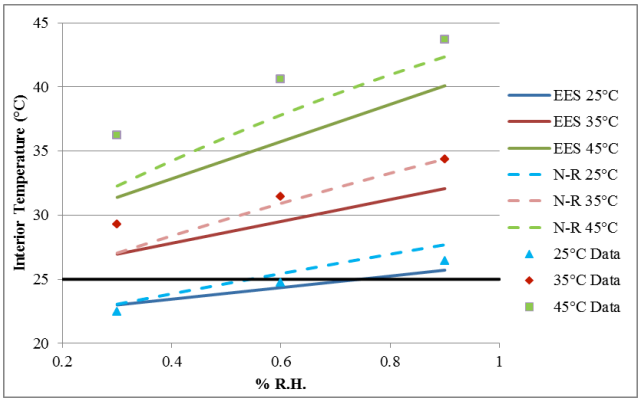

Figure 10 Copper calculation comparison with data points from post-helium tests

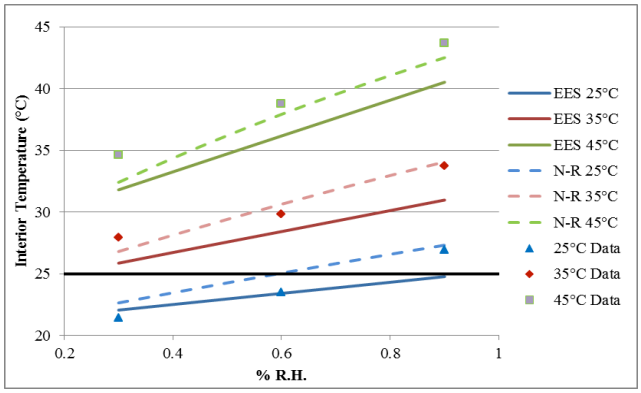

Figure 11 Aluminum calculation comparison with data points from post-helium test

The sealed boxes are the most thermally effective product developed or tested at both being approximately 0.9 effective. The aluminum box performs slightly better than the

copper box has a lower cost of the material. Regardless, both boxes are recommended for use at temperatures below up to 35 ^{o}C with relative humidities up to approximately 40%.

Table 6 Heat gain flux as a result of the door leaks or heat conducted into the front and back metal roof faces

T_{amb} (°C)	T_i (°C)	q_{gain} (W/m^{2}K)
25.25	21.95	129
34.45	28.65	226.7
44.45	35.45	351.7
25.75	24.15	62.53
34.95	30.65	168
44.35	39.65	183.7
25.35	26.65	-50.8
34.85	34.05	31.26
44.05	43.65	15.63

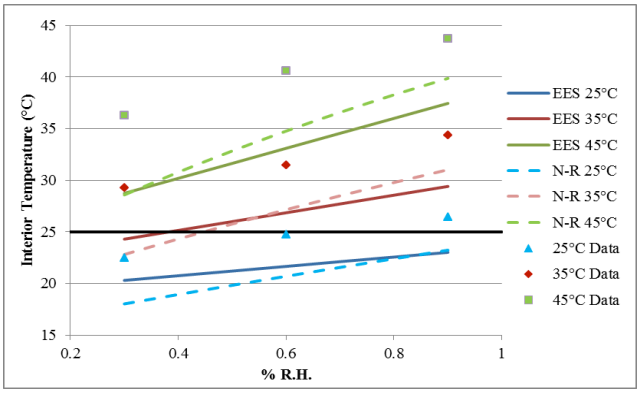

Figure 12 Copper thermal model calculations without gain flux

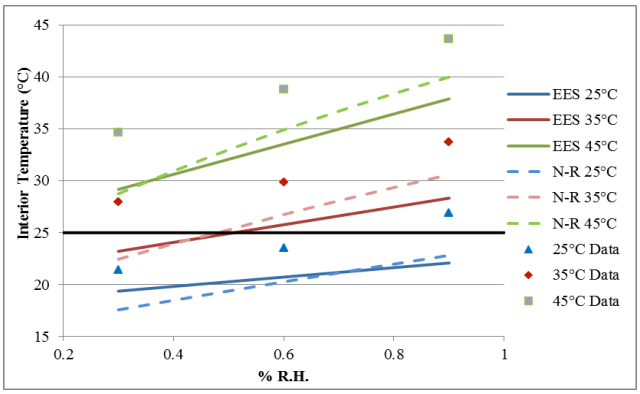

Figure 13 Aluminum thermal model calculations without gain flux

Life Cycle Assessment Results

A Life Cycle Inventory (LCI) is established in SimaPro using the values in Table 2. The LCI accounts for the materials used in the construction of the boxes and the processes (from earth extraction to retirement) required to get them in their workable form. Once the final product has been analyzed, the impact categories are defined and graphed in all the following figures.

The most prominent detriment was the zinc-coated steel angles used as the skeleton of the boxes. To eliminate the harm caused by this metal, the skeleton can be constructed out of wood. Wooden slabs are more sustainable and easier to procure in the intended countries of operation. If the wooden skeleton were utilized, the most unsustainable material would be the insulating foam sheets and gap filler.

The characterization comparison shows the environmental impacts of the two boxes based on their construction and use scenarios as a total percentage. The results show the relative contribution of the box LCI results to the impact category indicator results. Even though both roof metals were assumed to be recycled, the aluminum box is still showing a greater environmental impact. For all categories, the aluminum detriment can be attributed to the reworking process associated with recycling the metal to a thin sheet for the roof.

Normalization shows to what extent an impact category has a significant contribution to the overall environmental problem. It reduces the number of impact categories by allowing only the significant contributors of both boxes to remain and shows the order of magnitude of the environmental problems generated by the life cycle compared to the total environmental loads in Europe. Results show the aluminum box has the greatest detriment on the fossil fuel consumption, the carcinogens released and the respiratory organics. This can again be contributed to the aluminum processing techniques of recycled material.

CONCLUSION

Evaporative cooling is one of the only cost effective passive options available for use in malaria ridden countries. Utilizing a design developed by a previous team, several prototypes of passive cooling were built and tested with the goal of maintaining the box internal temperature at 25°C or below and store a sufficient number of RDTs for operation. Since the start of testing, there have been several modifications enacted that have proved to increase the cooling effectiveness. These included removing the cardboard sides, filling gaps and modifying the door. The post-helium sniffer tests illustrated that by reducing the leaks, the effectiveness of the boxes increased. If the boxes were manufactured with greater precision and ensured for proper sealing, the greatest possible cooling effect will occur at all ambient relative humidities up to 40% and at an ambient temperature of 25°C.

The top wicking evaporative box would meet both the requirements and objectives laid out above depending on the interior size and the quality of construction. The smaller box was ideal for housing at least 6 RDT units while the larger boxes housed at least 40 units with shelves. Through the course of testing, it was found that none of the boxes met the full requirements of the environmental conditions expected for operation of ambient temperature variance between 25-45°C. However for all temperatures up to 35°C and humidities up to approximately 40%, all the boxes kept the RDTs under the required temperature of 25°C. The smaller box showed greater efficiency in keeping the interior cooler than the larger boxes due to the greater surface area to volume ratio. It is therefore recommended that FIND utilize the smaller boxes or those with similar cooling surface to volume ratio design for rural clinics.

NOMENCLATURE

A	Area of heat transfer surface; total wetted surface area by wicking material	(m^2)
c_{pa}	Specific heat of ambient air	(J/kgK)
D_{ab}	Binary diffusion coefficient for water/air	(m^2/s)
h_{fg}	Heat of vaporization	(J/kg)
h_{hx}	Convective heat transfer coefficient	(W/m^2K)
h_m	Mass transfer coefficient	(m/s)
k_{air}	Air thermal conductivity	(W/mK)
k_{metal}	Metal thermal conductivity	(W/mK)
L	Characteristic length	(m)
Le	Lewis number	(dimensionless)
L_{pitch}	Roof pitch length	(m)
L_{side}	Box side length	(m)
Nu_L	Nusselt number	(dimensionless)
Pr	Prandtl number	(dimensionless)
q_{cond}	Conduction flux	(W/m^2)
q_{convec}	Convection flux	(W/m^2)
q_{evap}	Evaporation flux	(W/m^2)
q_{gain}	Heat gain flux	(W/m^2)
q_{rad}	Radiation heat flux	(W/m^2)
R_{cloth}	Contact and cloth thermal resistance	(m^2K/W)
R_{cond}	Thermal resistance of metal roof	(m^2K/W)
Ra_L	Rayleigh number	(dimensionless)
Re	Reynolds number	(dimensionless)
T_{amb}, T_∞	Ambient temperature	(K)
T_i	Internal temperature	(K)
T_s	Surface temperature	(K)
u	Air velocity	(m/s)
v_g	Specific volume of vapor	(m^3/kg)

Greek

α	Thermal diffusivity	(m^2/s)
β	Thermal expansion coefficient	(1/K)
ε	Cooling effectiveness	(dimensionless)
ε_{felt}	Cloth emissivity - felt	(dimensionless)
θ	Pitch angle	(deg)
μ	Air viscosity	(kg/m-s)
ν	Kinematic viscosity	(m^2/s)
ρ	Density	(kg/m^3)
σ	Stefan-Boltzman constant	(W/m^2K^4)
ϕ	Relative humidity	(decimal)

ACKNOWLEDGMENTS

The authors would like to acknowledge Dr. David Munoz for his support and assistance with this project. His guidance and expertise were vital in the completion of this research.

REFERENCES

[1] Aimiuwu, V. 1991. Evaporative cooling of water in hot arid regions. *Energy Conservation and management.* Vol. 33, No. 1. pp. 69-74.

[2] Anyanwu, E.E. 2004. Design and measured performance of a porous evaporative cooler for preservation of fruits and vegetables. *Energy Conservation and management*. Vol. 45. pp. 2187-2195.

[3] Camargo, J.R., C.D. Ebinuma, and J.L. Silveira. 2005. Experimental performance of a direct evaporative cooler operating during summer in a Brazilian city. *International Journal of Refrigeration*. Vol. 28, pp. 1124-1132.

[4] Enibe, S. 1997. Solar refrigeration for rural applications. *Renewable Energy*. Vol. 12, No. 2. pp. 157-167.

[5] Frigon, N., and D. Matthews. 1997. *Practical Guide to Experimental Design*. John Wiley & Sons, Inc.

[6] Ghosal, M.K, G.N. Tiwari, and N.S.L. Srivastava. 2003. Modeling and experimental validation of a greenhouse with evaporative cooling by moving water film over external shade cloth. *Energy and Buildings*. Vol. 35. pp. 843-850.

[7] Giabaklou, Z., and J.A. Ballinger. 1996. A Passive Evaporative Cooling System by Natural Ventilation. *Building and Environment.* Vol. 31, No. 6. pp. 503-507.

[8] Incropera, F., D.P. Dewitt, T.L. Bergman and A.S. Levine. 2007. *Fundamentals of Heat and Mass Transfer*. John Wiley & Sons, Inc.

[9] Kim, D.S. and C.A. Infante Ferreira. 2008. Solar refrigeration options - a state-of-the-art review. *International Journal of Refrigeration*. Vol. 31, pp. 3-15.

[10] Maerefat, M., and A.P. Haghighi. 2010. Natural cooling of stand-alone houses using solar chimney and evaporative cooling cavity. *Renewable Energy*. Vol. 35, pp. 2040-2052.

[11] Montgomery, D.C. 1997. *Design and Analysis of Experiments*. John Wiley & Sons, Inc.

[12] Mulder, K. 2006. *Sustainable Development for Engineers: A Handbook and Resource Guide*. Greenleaf Publishing.

[13] Munoz, D., J. Hutsell and J. Vajdic. 2009. *Report for Field Study 1: Kampala & Gulu, Uganda, Mungao Sublocation, Kenya*.

[14] Otto, K. and K. Wood. 2001. *Product Design: techniques in Reverse Engineering and New Product Development.* Prentice Hall, Inc.

[15] Sonntag, R. C. Borgnakke, and G.J. Van Wylen. 2003. *Fundamentals of Thermodynamics*. John Wiley & Sons, Inc.

[16] Srivastava, A. and G.N. Tiwari. 1984. Experimental Validation of a thermal model of an evaporative cooling system. *Energy Convers. Mgmt*. Vol. 24, No. 4. pp. 305-311.

[17] Thepa, S., K. Kiritikara, J. Hirunlabh and J. Khedari. 1999. Improving indoor conditions of a Thai-style mushroom house by means of an evaporative cooler and continuous ventilation. *Renewable Energy*. Vol. 17. pp. 359-369.

[18] White, F. 2008. *Fluid Mechanics*. Sixth Edition. McGraw Hill Publishers.